Journal of Alloys and Compounds 515 (2012) 134–142

Contents lists available at SciVerse ScienceDirect

Journal of Alloys and Compounds

journal homepage: www.elsevier.com/locate/jallcom

Dielectric dispersion and spectroscopic investigations on Na_2SO_4–B_2O_3–P_2O_5 glasses mixed with low concentrations of TiO_2

A.V. Ravi Kumar[a,b], Ch. Srinivasa Rao[b], T. Srikumar[b], Y. Gandhi[a], V. Ravi Kumar[a], N. Veeraiah[a,*]

[a] Department of Physics, Acharya Nagarjuna University – Nuzvid Campus, Nuzvid 521201, A.P., India
[b] Department of Physics, Andhra Loyola College, Vijayawada 520008, A.P., India

ARTICLE INFO

Article history:
Received 17 November 2011
Received in revised form
23 November 2011
Accepted 23 November 2011
Available online 2 December 2011

Keywords:
Na_2SO_4–B_2O_3–P_2O_5 glasses
Titanium ions
Dielectric properties
Spectroscopic properties

ABSTRACT

A series of Na_2SO_4–B_2O_3–P_2O_5 glasses doped with different concentrations of TiO_2 (0 to 1.0 mol%) have been synthesized. Dielectric properties (over a range of frequency and temperature) and a variety of spectroscopic (optical absorption, IR, Raman and ESR) properties of these glasses have been investigated. The values of dielectric parameters viz., dielectric constant, loss and ac conductivity at any frequency and temperature are observed to increase with the concentration of TiO_2. The optical absorption and ESR spectral studies have pointed out that a part of titanium ions do exist in Ti^{3+} state in addition to Ti^{4+} state especially in the samples containing higher concentration of TiO_2. The increase of dielectric constant with the concentration of TiO_2 is explained on the basis of space charge polarization due to increasing concentration of various bonding defects in the glass network. The dielectric relaxation effects exhibited by these glasses are quantitatively analyzed by pseudo Cole–Cole method and the spreading of relaxation times is established. The ac conductivity is observed to increase with increasing content of TiO_2, the mechanism responsible for such increase is well explained based on the modifying action of Ti^{3+} ions.

1. Introduction

Alkali sulfate mixed phosphate glasses are being used to immobilize radioactive waste for long time safe storage [1]. These glasses are also proved to be suitable for their application in micro batteries, smart card, medical appliance [2,3]. These materials exhibit high electrical conductivity (purely ionic), compatible with the electrode materials and are thermally and chemically stable. The SO_4^{2-} ions largely dissolve in the phosphate glass matrix and mostly remain as isolated units [4]. However, there are also reports suggesting that sulfate ions and metaphosphate ions interact weakly and form a small dynamic concentration of dithiophosphate (DTP) units in the glass matrices [5]. Such weak and variable interaction between these two ions is expected to influence the electrical properties to a large extent. A considerable number of previous studies on a variety of physical properties of different alkali sulfophosphate glasses are available in the literature [6–9]. The introduction of B_2O_3 to alkali sulfophosphate glasses is expected to increase the thermal stability of the glass network (since borate groups form $M^+[BO_4]^-$ pairs) and also reported to increase the electrical conductivity [10–13].

The chemical inertness, thermal stability and also electrical properties of alkali borosulfophosphate glasses can further be improved by mixing a small quantity of TiO_2 to the glass matrix. The addition of TiO_2 further makes borosulfophosphate glasses suitable for applications in non-linear optical devices, integrated circuits and low loss optical waveguides [14]. Kityk and his co-workers have reported extensive studies on non-linear optical (NLO) properties of similar type of glass systems. Their studies have yielded valuable information which will be useful for considering these types of glasses for optically operated NLO devices [15,16].

Normally, the ions of titanium exist in the glass in Ti^{4+} state and participate in the glass network forming with TiO_4, TiO_6 and some times with TiO_5 (comprising of trigonal bipyramids) structural units [14,17]. However, there are also reports suggesting that these ions may also exist in Ti^{3+} valence state in some of the glass matrices and acts as modifiers [17,18]; such variation in the coordination and valence of titanium ions are expected to cause the structural modifications and local field variations in the glass network and expected to influence the electrical properties to a large extent.

In this investigation we have studied the influence of titanium ions on dielectric and ac conductivity properties of Na_2SO_4–B_2O_3–P_2O_5 glasses. To have some pre-assessment over the structural aspects of the glasses which may help for clear understanding of the dielectric properties, we have also undertaken the studies on optical absorption, ESR and IR studies.

* Corresponding author. Tel.: +91 8656 235551; fax: +91 8656 235551.
E-mail address: nvr8@rediffmail.com (N. Veeraiah).

0925-8388/$ – see front matter © 2011 Elsevier B.V. All rights reserved.
doi:10.1016/j.jallcom.2011.11.126

Table 1
Physical parameters of Na_2SO_4–B_2O_3–P_2O_5: TiO_2 glasses.

Physical parameter↓	Glass →					
	T_0	T_2	T_4	T_6	T_8	T_{10}
Density d (g/cm^3)	2.5556	2.5609	2.5678	2.5776	2.5844	2.5876
Dopant ion conc. N_i ($\times 10^{20}$ ions/cm^3)	–	0.25	0.51	0.77	1.03	1.29
Interionic distance R_i (Å)	–	33.98	26.94	23.49	21.32	19.77
Polaron radius R_p (Å)	–	13.69	10.89	9.47	8.59	7.97
Field strength F_i (10^{15}, cm^{-2})	–	0.16	0.25	0.33	0.41	0.47

2. Experimental

The detailed compositions of the glasses used in the present study are as follows:

T_0: $40.0Na_2SO_4$–$30B_2O_3$–$30P_2O_5$
T_2: $39.8Na_2SO_4$–$30B_2O_3$–$30P_2O_5$: $0.2TiO_2$
T_4: $39.6Na_2SO_4$–$30B_2O_3$–$30P_2O_5$: $0.4TiO_2$
T_6: $39.4Na_2SO_4$–$30B_2O_3$–$30P_2O_5$: $0.6TiO_2$
T_8: $39.2Na_2SO_4$–$30B_2O_3$–$30P_2O_5$: $0.8TiO_2$
T_{10}: $39.0Na_2SO_4$–$30B_2O_3$–$30P_2O_5$: $1.0TiO_2$

Analytical grade reagents of H_3BO_3, Na_2SO_4, P_2O_5 and TiO_2 powders in appropriate amounts (all in mol%) were thoroughly mixed in an agate mortar, calcinated at about 900 °C for 2 h in a platinum crucible and subsequently melted in the temperature range of 1200–1250 °C in an automatic temperature controlled furnace for about 30 min. The resultant bubble free melt was then poured in a pre-heated brass mould and annealed at 350 °C. The samples prepared were mechanically ground and optical polished to the dimensions of 1 cm × 1 cm × 0.2 cm. The amorphous state of the samples was verified by XRD and scanning electron microscope studies. Differential thermal analysis (DTA) was carried out in the temperature range 30–1000 °C using Netzsch Simultaneous DSC/TG Thermal Analyzer (STA409C) to determine the glass transition temperature. The heating rate was maintained as 10 °C/min and the values of T_g (glass transition temperature) and T_c (crystallization temperature) were evaluated to an accuracy of ±1.0 °C. The density of the glasses was determined to an accuracy of (±0.0001) by the standard principle of Archimedes' using o-xylene (99.99% pure) as the buoyant liquid. The mass of the samples was measured to an accuracy of 0.1 mg using Ohaus digital balance Model AR2140 for evaluating the density. Infrared transmission spectra were recorded on a JASCO-FTIR-5300 spectrophotometer to an accuracy of 0.1 cm^{-1} in the spectral range 400–2000 cm^{-1} using potassium bromide pellets (300 mg) containing pulverized sample (1.5 mg). These pellets were pressed in a vacuum die at ~680 MPa. The ESR spectra of the fine powders of the samples were recorded at room temperature on E11Z Varian X-band (ν = 9.5 GHz) EPR spectrometer. The g value of the signals is evaluated to an accuracy of ±0.001.

The optical absorption spectra of the glasses were recorded to a resolution of 0.1 nm at room temperature in the spectral wavelength range covering 300–1000 nm using JASCO Model V-670 UV-vis-NIR spectrophotometer. The dielectric measurements were carried out on LCR Meter (Hewlett-Packard Model-4263 B) in the frequency range 10^2–10^5 Hz and in the temperature range 30–300 °C. The accuracy in the measurement of dielectric constant is ~0.001 and that of loss is ~10^{-4}.

3. Results

The physical parameters such as titanium ion concentration N_i, mean titanium ion separation R_i and polaron radius R_p were evaluated from the measured values of density d and calculated average molecular weight $\overline{M}$ using the conventional formulae [19] and are furnished in Table 1.

In Fig. 1, DTA scan for Na_2SO_4–B_2O_3–P_2O_5 glasses doped with 0.6 mol% of TiO_2 is presented; the thermogram exhibited a typical glass transition with the inflection point at about 415 °C following by an exothermic peak due to crystallization at about 810 °C. With the increasing content of TiO_2 in the glass matrix, the glass transition temperature is observed to decrease (inset of Fig. 1). The value of ($T_c - T_g$), a parameter that represents thermal stability of glass against devitrification, is found to decrease with the content of TiO_2 (inset of Fig. 1).

Fig. 2(a) presents optical absorption spectra of Na_2SO_4–B_2O_3–P_2O_5: TiO_2 glass samples recorded at room temperature in the wavelength region 300–1000 nm. The absorption edge for TiO_2 free glass is identified at 288 nm where as for the glass T_2, it is observed at 312 nm. As the concentration of TiO_2 is increased the edge exhibited red shift. Additionally, the spectrum of glass T_2 exhibited two clearly resolved absorption bands at 516 and 691 nm. As the concentration of TiO_2 is continued to increase, the half width and intensity of these two bands are observed to increase with the shifting of the peak positions towards slightly longer wavelength (Table 2).

From the observed absorption edges, we have evaluated the optical band gaps (E_o) of these samples by drawing Tauc plots (Fig. 2(b)) between $(\alpha\hbar\omega)^{1/2}$ and $\hbar\omega$ as per the equation [20]:

$$\alpha(\omega)\hbar\omega = c(\hbar\omega - E_o)^2 \quad (1)$$

A considerable part of each of these curves is observed to be linear indicating that Eq. (1) is valid. The validity of this quadratic equation points out that the optical band gap is caused by amorphous optical absorption edge. Some deviations observed from this dependence may be due to trapping by disordered states within the energy gap.

From the extrapolation of the linear portion of the curves of Fig. 2(b), the value of optical band gap (E_o) is determined and its variation with the concentration of TiO_2 is shown as the inset of Fig. 2(b); the variation of E_o with the content of TiO_2 exhibited a decreasing trend.

ESR spectra of Na_2SO_4–B_2O_3–P_2O_5: TiO_2 glasses doped with different concentrations of TiO_2 recorded at room temperature are presented in Fig. 3. The spectrum of glass T_2 consists of an intense asymmetric spectral line centered at about g = 1.970. The half width and the intensity of this signal exhibited a gradual increase with the concentration of TiO_2. The intensity ($\Im$) of the ESR signal, assumed

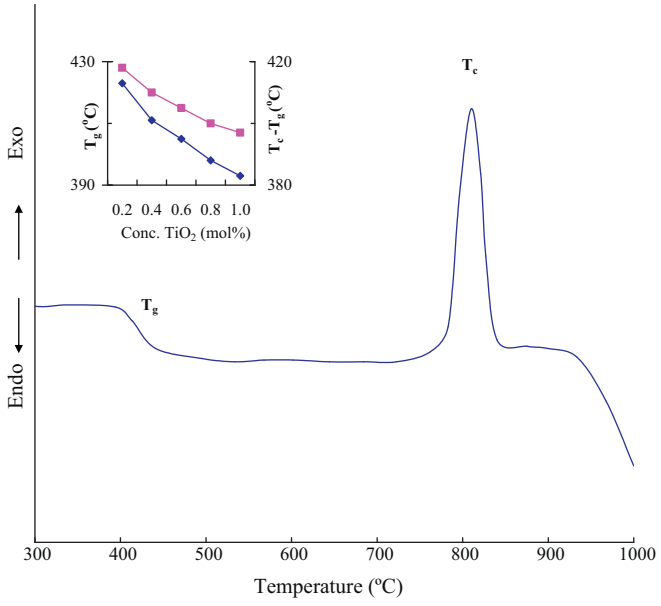

Fig. 1. DTA trace of T_6 glass. Inset shows the variation of T_g and $T_c - T_g$ with the concentration of TiO_2.

Table 2
Data on optical absorption spectra Na_2SO_4–B_2O_3–P_2O_5: TiO_2 glasses.

Glass	Cut-off wavelength (nm)	Band positions (nm)		Optical band gap (eV)
		$^2B_{2g} \rightarrow {}^2B_{1g}$	$^2B_{2g} \rightarrow {}^2A_{1g}$	
T_0	292	–	–	4.25
T_2	318	509	678	3.90
T_4	325	516	691	3.82
T_6	329	524	698	3.77
T_8	331	527	700	3.75
T_{10}	354	532	706	3.50

to be proportional to the product of the peak-to-peak height (I) and the square of its width (ΔB)

$$\Im \approx I(\Delta B)^2, \quad (2)$$

is evaluated and its dependence with the concentration of TiO_2 is shown as an inset of Fig. 3. The figure shows that the intensity of the resonance signal increases with increase in the concentration of TiO_2.

The IR spectra (Fig. 4) of Na_2SO_4–B_2O_3–P_2O_5: TiO_2 glasses exhibited conventional vibrational bands due to phosphate groups in the regions 1277–1295 cm^{-1} (anti-symmetrical vibrations of PO_2^- groups/P═O stretching vibrations), 1085–1106 cm^{-1} (a normal vibrational mode of PO_4^{3-} group arising out of ν_3 – symmetric stretching), 927–944 cm^{-1} (P—O—P asymmetric bending vibrations/this region may also consist of bands due to pyrophosphate groups $P_2O_7^{4-}$) and another band in the region of 760–790 cm^{-1} due to P—O—P symmetric stretching vibrations [21]. The spectra have also exhibited three usual bands originated from borate groups in the regions 1381–1414 cm^{-1} due to BO_3 units, 944–964 cm^{-1} due to BO_4 units and 709–724 cm^{-1} due to bending vibrations of B—O—B linkages [22]. In the spectral regions 658–678 cm^{-1} and 1124–1148 cm^{-1} vibrational bands corresponding to bending and asymmetric modes of SO_4^{2-} groups, respectively are also observed [23,24]; additionally a prominent band in the regions 581–620 cm^{-1} attributed to the vibrations of TiO_6 structural units [25–27] is also located in these spectra. With the gradual introduction of TiO_2 in the glass network, all the asymmetrical bands are observed to grow at the expense of symmetrical bands. The band due to Ti—O—Ti symmetric stretching vibrations of TiO_4 units is also expected in the region of P—O—P symmetric stretching vibrations (at about 760 cm^{-1}). The pertinent data related to IR spectra are presented in Table 3.

The dielectric constant ε' and loss $\tan\delta$ at room temperature (≈30 °C) of TiO_2 free Na_2SO_4–B_2O_3–P_2O_5 glasses at 1 kHz are measured to be 10.8 and 0.004, respectively. With increase in the concentration of TiO_2 in the glass matrix, these values are observed to increase considerably. Fig. 5 represents the temperature dependence of ε' at 1 kHz of Na_2SO_4–B_2O_3–P_2O_5 glasses doped with different concentrations of TiO_2 and the dependence of ε' with temperature at different frequencies for the glass T_2 is shown an inset of the same figure. The value of ε' exhibited a considerable increase at higher temperatures especially at lower frequencies; the rate of increase of ε' with temperature at any frequency is found to increase with increase in the concentration of TiO_2.

Fig. 6(a) represents a comparison plot of variation of $\tan\delta$ with temperature, measured at a frequency of 10 kHz for Na_2SO_4–B_2O_3–P_2O_5 glasses doped with different concentrations of TiO_2. Fig. 6(b) represents the temperature dependence of $\tan\delta$ of glass T_6 at different frequencies.

Variation of $\tan\delta$ with temperature have exhibited distinct maxima; with increase in frequency, the temperature maximum of $\tan\delta$ shifts towards higher temperatures and with increase in temperature, the frequency maximum shifted towards higher frequencies, such variation indicates the relaxation character of dielectric losses in these glass [28]. The full width at half maximum (FWHM) and the peak value $(\tan\delta)_{max}$ of the relaxation curve (that represent the strength of the relaxation character) are observed to increase gradually with the content of TiO_2. Using the relation:

$$f = f_o \exp\left(\frac{-W_d}{k_B T}\right), \quad (3)$$

the effective activation energy, W_d, for the dipoles is evaluated for the glasses doped with different concentrations of TiO_2. In Eq. (3), f is the relaxation frequency, k_B is the Boltzmann constant, T is absolute temperature and f_o is a constant. The activation energy W_d is found to decrease with increase in the concentration of TiO_2 (Table 4).

The ac conductivity σ_{ac} is calculated at different temperatures using the equation:

$$\sigma_{ac} = \omega\varepsilon'\varepsilon_o \tan\ \delta, \quad (4)$$

(where ε_o is the vacuum dielectric constant and ω is the angular frequency) for different frequencies and the plot of $\log\sigma_{ac}$ against $1/T$ for all the glasses at 100 kHz is shown in Fig. 7; the conductivity is found to increase considerably with increase in the concentration of TiO_2 at any given frequency and temperature. From these plots, the activation energy for the conduction in the high temperature region is evaluated and presented in Table 4 along with other pertinent data.

4. Discussion

The composition of Na_2SO_4–B_2O_3–P_2O_5: TiO_2 glass system is an admixture of glass formers, modifiers and intermediates. P_2O_5 is a strong glass forming oxide, participates in the glass network with PO_4 structural clusters. The PO_4 tetrahedra are linked together with covalent bonding in chains or rings by bridging oxygen. Neighboring phosphate chains are linked together by cross-bonding between the metal cation and two non-bridging oxygen atoms of each PO_4 tetrahedron [29]. The presence of such PO_4 units in the titled glass samples is evident from the IR spectral studies. B_2O_3 is also a strong glass former, when it is mixed in the phosphate glasses, the tetrahedral boron entities dominate in the phosphate-rich domain where as trigonal boron entities prevail in the borate-rich side and form easily B—O—P bridges. The highest stability occurs for fully polymerized glasses and can be related to the energetics of the reaction B—O—B + P—O—P = 2(B—O—P); this relation also suggests that the B—O—P linkage is more stable relatively than the mixture of B—O—B and P—O—P linkages [30–33].

With the addition of Na_2SO_4 a gradual depolymerization of the phosphate chains and formation of short phosphate units take place. During this process the sulfate units remain as terminal groups without any chemical interaction with the phosphate units [4]. As a consequence, variation in the density is hardly expected with the variation in the content of Na_2SO_4; however, due to the formation of dithiophosphate (DTP) units (due to the weak interaction between pyrophosphates), a slight increase in the density is possible (Table 1). Normally the phosphate network contains

Table 3
Data on infrared spectra Na_2SO_4–B_2O_3–P_2O_5: TiO_2 glasses recorded at room temperature (assignment of band positions in cm^{-1}).

Glass sample	BO_3 units	PO^{2-} asym.	SO_4^{2-} units		P—O—P asym. stretching	PO_4^{3-} groups/BO_4 units	P—O—P sym. stretch. & TiO_4 units	B—O—B linkages	TiO_6 units
			ν_1	ν_2					
T_2	1414	1295	1148	658	1085	944	762	709	620
T_4	1405	1291	1146	664	1092	953	772	713	612
T_6	1398	1286	1141	669	1094	958	779	717	601
T_8	1390	1282	1135	671	1101	962	783	719	592
T_{10}	1381	1277	1124	678	1106	964	797	724	581

Table 4
Summary of data on dielectric loss of Na_2SO_4–B_2O_3–P_2O_5: TiO_2 glasses.

Glass	$(\tan\delta)_{max.avg}$	Temp. region of relaxation (°C)	A. E. for dipoles (eV) (±0.01)	Spreading factor β	A. E. for conduction (eV) (±0.01)	Exponent, *s*
T_2	0.050	113–158	0.65	0.46	0.81	0.65
T_4	0.061	97–147	0.62	0.48	0.79	0.70
T_6	0.078	90–140	0.59	0.50	0.76	0.73
T_8	0.126	79–128	0.56	0.53	0.70	0.77
T_{10}	0.161	68–118	0.53	0.55	0.67	0.81

$[POO_{2/2}O]^-$ (phosphate tetrahedra with one bridging oxygen) and $[POO_{1/2}O_2]^{2-}$ (phosphate tetrahedra with two bridging oxygen) structural groups [5] as shown below:

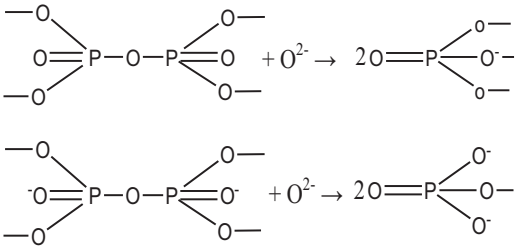

Out of these two ions, it is the $[POO_{2/2}O]^-$ ion that interacts with sulfate ion and form SPO_7^{3-} (dithiophosphate) specie [22]. However there are some affirmative reports (based on Raman and NMR investigations) on sulfophosphate glasses suggesting that SO_4^{2-} species do not contribute to network formation and instead these groups participate in the depolymerization of the phosphate network similar to Ti^{3+} and Na^+ ions [34].

Titanium ions exist mainly in Ti^{4+} state in Na_2SO_4–B_2O_3–P_2O_5 glass network. Nevertheless, the reduction of Ti^{4+} to Ti^{3+} is unavoidable during melting at high temperatures and annealing processes of the glasses. Ti^{4+} ions occupy both tetrahedral and substitutional octahedral sites as corner-sharing $[TiO_6]^{2-}$ units where as Ti^{3+} ions occupy only modifying positions and depolymerize the glass network. TiO_4 and TiO_6 units of Ti^{4+} ions enter the glass network and form linkages of the type P—O—Ti and B—O—Ti.

In detail the interaction of TiO_2 with phosphate, borate and borophosphate networks may be represented as follows:

(i) $P_2O_5 \equiv 2[POO_{3/2}]$; $TiO_2 \equiv [TiO_{4/2}]$; $TiO_2 + 2[POO_{3/2}] \Rightarrow [TiO_{6/2}]^{2-}$

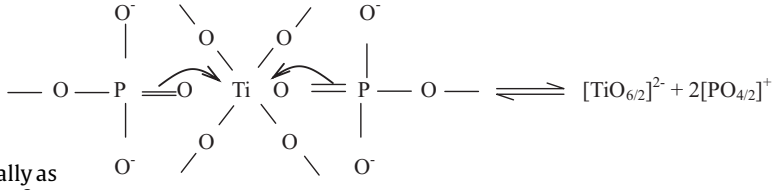

$+ 2[PO_{4/2}]^+$ and diagramatically as

(ii) $B_2O_3 + 2TiO_2 + 2O_2 \rightarrow 2[BO_{6/2}]^3 + [TiO_{4/2}] + [TiO_{6/2}]$

(iii) $B_2O_3 + 3TiO_2 + 2P_2O_5 + O_2 \rightarrow 2[BO_{6/2}]^3 + 4[PO_{4/2}]^+ + 2[TiO_{4/2}] + [TiO_{6/2}]$

These equations clearly suggest that incorporation of the Ti ions into the glass network leads to some d–p charge transfer between the 3d Ti ions and the surrounding ligands.

T_g and $T_c - T_g$ values evaluated from DTA traces show a decreasing trend with increase in the concentration of TiO_2. Such trend indicates the decrease of augmented cross-link density of various structural groups and closeness of packing. This is possible only if there is a gradual increasing proportion of Ti^{3+} ions that act as modifiers in the glass network.

The electronic configuration of Ti^{3+} ion is $3d^1$. In octahedral field or tetrahedral field, the ground state ^2D of the $3d^1$ ion splits into ^2E and $^2T_2$ states. In the tetragonally distorted octahedral field, the $^2T_2$ state further splits into three $^2B_{2g}$ (viz., $|xy\rangle$, $|yz\rangle$ and $|zx\rangle$) states, whereas, the ^2E excited state splits into $A_{1g}\left|3z^2 - r^2\right\rangle$ and $B_{1g}\left|x^2 - y^2\right\rangle$ states. For d^1 ions in tetragonally compressed octahedron, the ground state is $B_{2g}|xy\rangle$. Hence, the bands observed in the optical absorption spectra at about 540 nm and 690 nm of the studied glass are assigned to $^2B_{2g} \rightarrow {}^2B_{1g}$ and $^2B_{2g} \rightarrow {}^2A_{1g}$ transitions of the Ti^{3+} ions, respectively [35,36]. With increase in concentration of TiO_2, a gradual growth of these two bands could clearly be seen; this observation indicates that there is an increasing fraction of Ti^{3+} ions in the glass network.

The octahedrally coordinated Ti^{3+} ions, similar to Na^+ ions, act as modifiers and are expected to induce non-bridging oxygen (NBO's) in the glass network. The analysis of IR spectral results have also indicated that, in the samples containing higher concentration of TiO_2, the asymmetric vibrational bands of phosphate groups dominate over symmetric bands. These factors indicate an increase in the concentration of NBO's in the glass network with increase in the concentration of TiO_2. Because of these reasons an increase in the degree of localization of electrons there by an increase in the donor centers in the glass network is possible. The presence of higher concentration of these donor centers decreases the optical band gap and shifts the absorption edge gradually towards higher

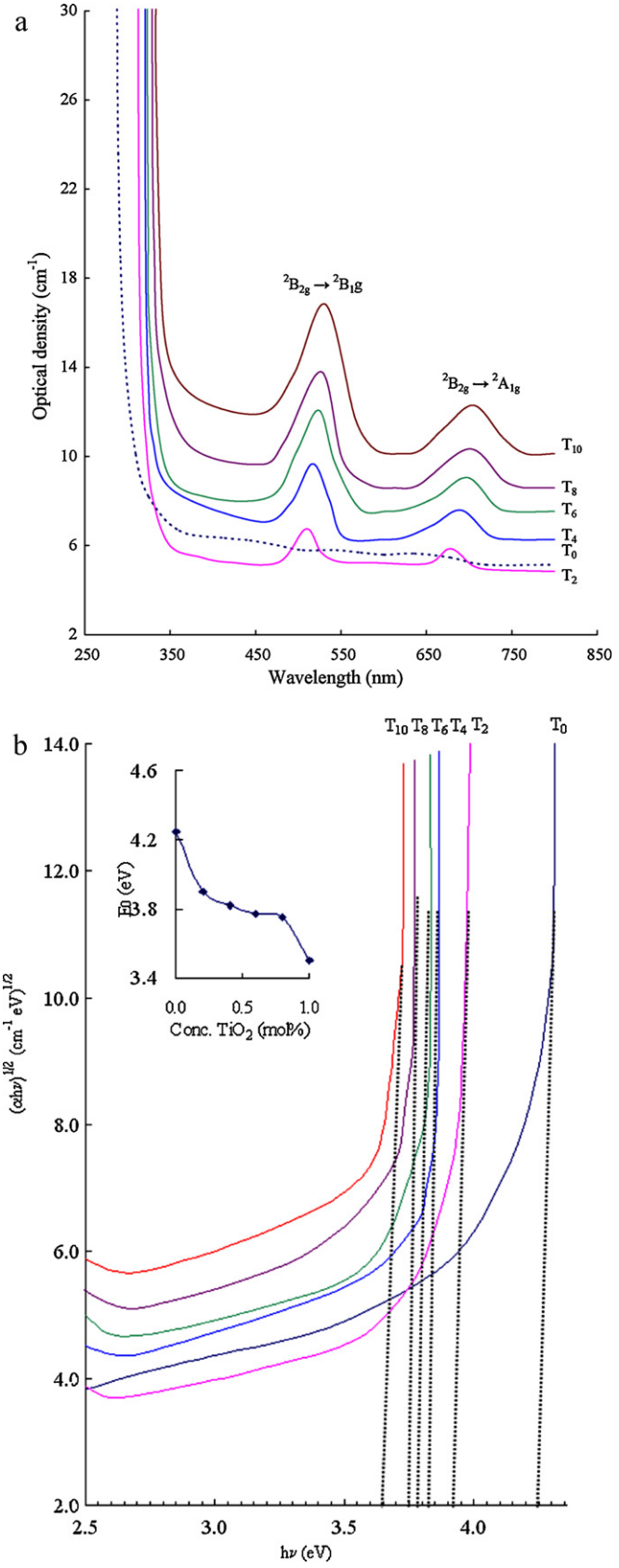

Fig. 2. (a) Optical absorption spectra of Na_2O_4–B_2O_3–P_2O_5: TiO_2 glasses. (b) Tauc plots of Na_2O_4–B_2O_3–P_2O_5: TiO_2 glasses. Inset shows the variation of optical band gap with the concentration of TiO_2.

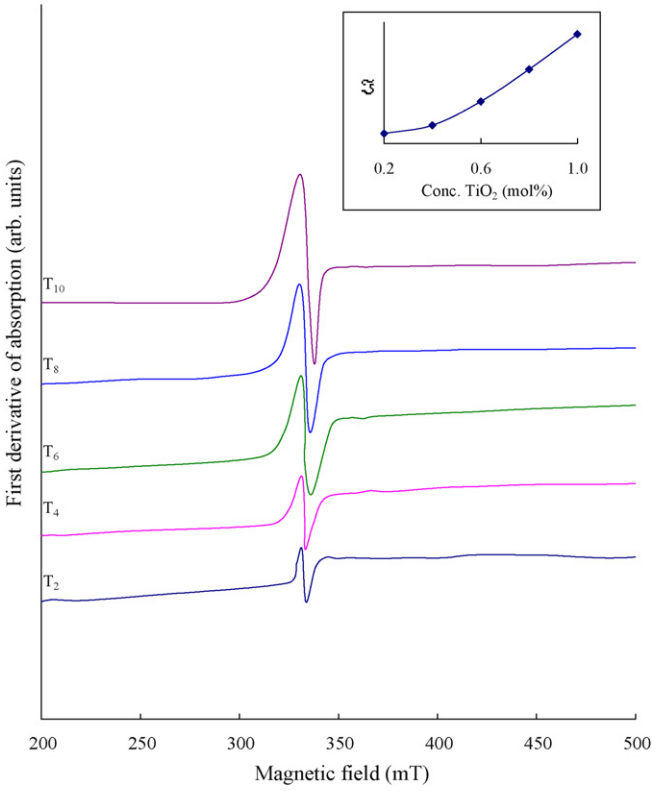

Fig. 3. ESR spectra of Na_2O_4–B_2O_3–P_2O_5: TiO_2 glasses recorded at room temperature. Inset shows the variation of intensity of the signal with concentration of TiO_2.

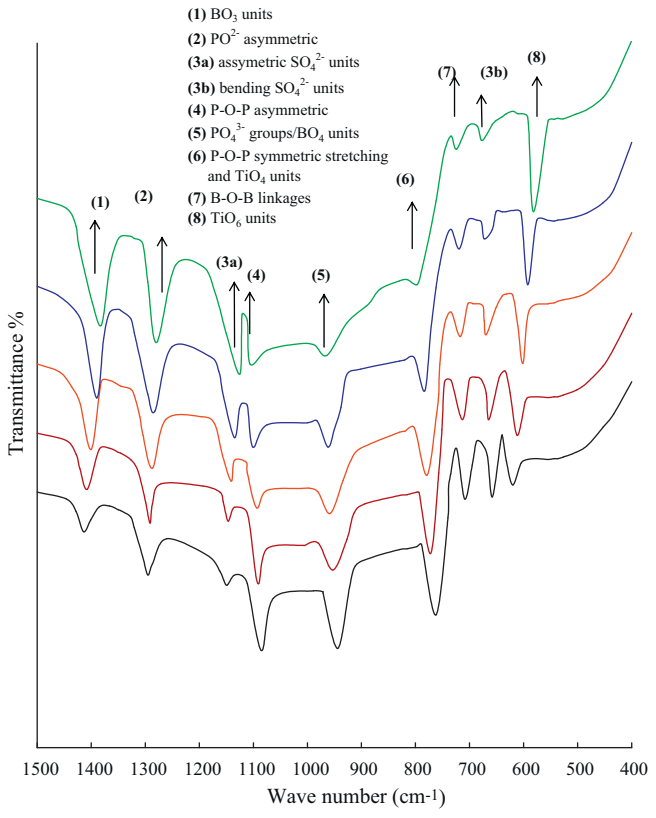

Fig. 4. IR spectra of Na_2O_4–B_2O_3–P_2O_5: TiO_2 glasses.

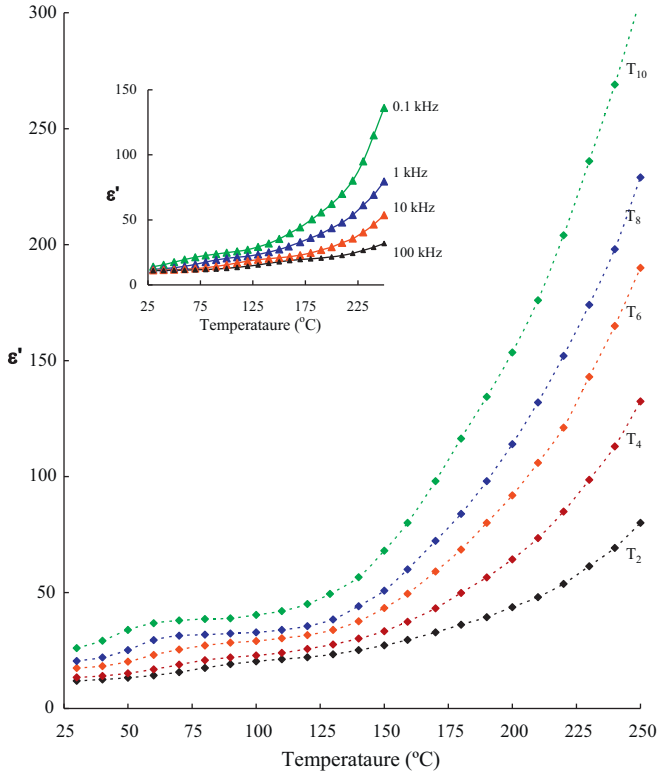

Fig. 5. A comparison plot of variation of dielectric constant with temperature at 1 kHz for Na_2O_4–B_2O_3–P_2O_5: TiO_2 glasses. Inset gives the variation of dielectric constant with temperature at different frequencies of glass T_2.

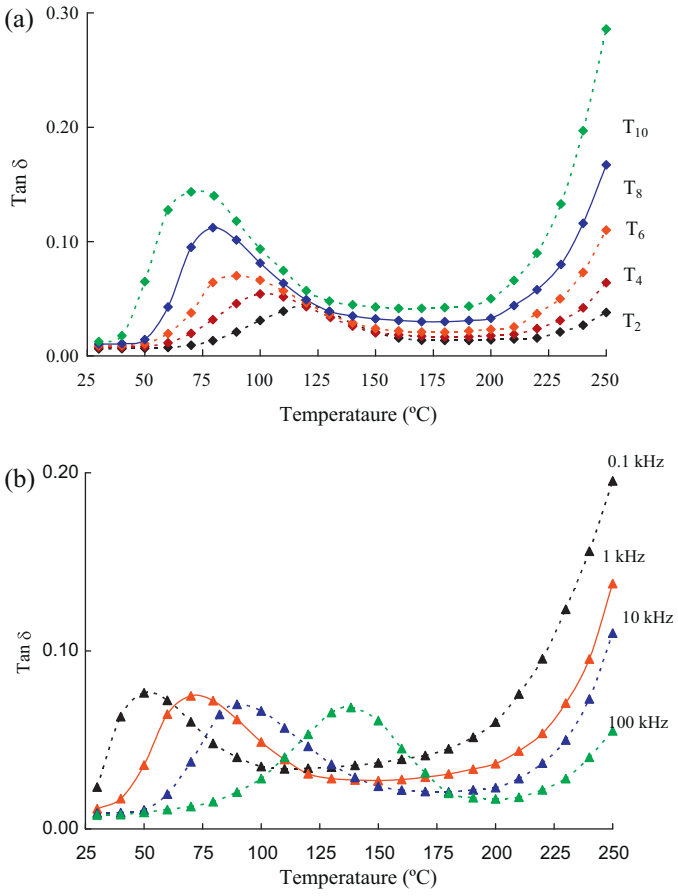

Fig. 6. (a) A comparision plot of variation of tan δ with temperature at 10 kHz for Na_2O_4–B_2O_3–P_2O_5: TiO_2 glasses. (b) The variation of tan δ with temperature at different frequencies of glass.

wavelength side. The gradual decrease in the proportion of network forming Ti^{4+} ions in the glass network leads to an increase in the generation of donor centers; as a consequence, there will be an increasing overlap between empty 3d states of Ti^{4+} sites and the neighboring excited states of localized electrons originally trapped on Ti^{3+} ions. Such overlap facilitates for the shrinkage of optical band gap and hence there is a decrease of optical band gap with increase in the content of TiO_2, as observed (Table 3).

In other words, the 3d levels of Ti ion within the effective energy gap will be influenced by bonding-anti-bonding of 2p O-2p B and s Pb levels to a large extent and contribute for the observed decrease of optical band gap.

The optical activation energy associated with the octahedral band of Ti^{3+} ions viz., $^2B_{2g} \rightarrow {}^2B_{1g}$ is decreased from 2.44 eV to 2.32 eV with the increase in the concentration of TiO_2 from 0.2 to 1.0 mol% (Table 2); this is clearly a characteristic signal of inter valence transfer or a polaronic type of absorption. To be more specific, the associated electrons are trapped at shallow sites within the main band gap. In terms of polaronic perception, this kind of situation is only possible if the local potential fluctuation is small as compared to the transfer integral, *j*. A small overlap between electronic wave-functions (corresponding to adjacent sites) due to strong disorder is contributive to polaron formation. So in terms of the polaron exchange the variation of optical band gap can be explained as fallows: the electron delivered by the impurity atom at the Ti^{4+} site converts this into a lower valence state Ti^{3+} and at the next stage, the trapped electron at this Ti^{3+} site is transferred to the neighboring new Ti^{4+} site by absorbing a photon energy. Thus the optical absorption in the glass samples is dominated by polaronic transfer between the Ti^{3+} and Ti^{4+} species [37,38].

In the ESR spectra, the central line observed at $g = 1.987$ is due to tetragonally compressed octahedral excitations of Ti^{3+} ions from the ground state $|xy\rangle$ [39,40]. The observed increase of intensity and half-width of the signal with the increase in the content of TiO_2 suggests a gradual increase in the concentration of Ti^{3+} ions in the glass network.

The other factors, e.g., the jumping frequency of the charge carriers (from Ti^{3+} to Ti^{4+}) which is proportional to exp $(-W/kT)$ also accounts for such variations. Here $W = 1/2W_D$ (mean energy difference between adjacent titanium ion sites) + W_H (the activation energy for the hopping process of the polarons between two identical sites). As the concentration of TiO_2 is increased gradually, the jumping rate of the polaron increases. This fact, together with the increasing concentration of the Ti^{3+} accounts for the increasing intensity of the ESR signal.

The IR spectral studies have revealed the intensity of the bands due to asymmetric vibrations of phosphate groups and also BO_3 groups grow at the expense of symmetrical bands of phosphate and BO_4 groups with increase in the content of TiO_2. Such variations suggest increasing modifying action of titanium ions by creating larger number NBO's in the glass network. As a result, the phosphate coordination reduces from four fold to three fold, two fold and even to one dimensional and the depolymerization of P—O—P, B—O—B, P—O—B and also P—O—Ti chains takes place and the strength of the glass network decreases. Thus the results of IR spectral studies point out that, there is growing degree of disorder in the glass network with the increase in the concentration of TiO_2.

The dielectric parameters viz., ε', tan δ and σ_{ac} are found to increase with increase in temperature for all the studied glasses. Further, at any frequency and temperature these parameters are found to increase with increase in the content of TiO_2 in the glass matrix. In general electronic, ionic, dipolar and space charge

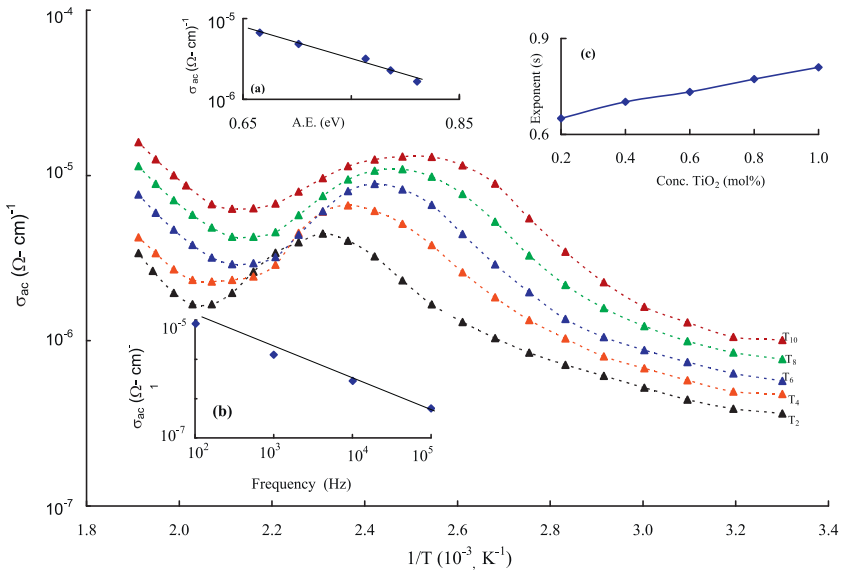

Fig. 7. Variation of sac with $1/T$ at 100 kHz of Na_2O_4–B_2O_3–P_2O_5: TiO_2 glasses. Inset (a) represents the variation of ac conductivity with activation energy, (b) variation of ac conductivity with different frequencies for the sample T_6 and (c) variation of exponent with the concentration of TiO_2.

polarizations contribute to the dielectric constant. Among these, it is the space charge polarization (which depends up on concentration defects in the glass network) that influences strongly the dielectric constant at lower frequencies. As mentioned earlier, the Ti^{3+} ions similar to Na^+ ions act as modifiers and create dangling bonds and non bridging oxygen ions by disrupting P—O—P, B—O—B, P—O—B, P—O—Ti and B—O—Ti linkages. In view of this, the glass network consists of $[SO_4]^{2-}$, $[POO_{1/2}O_2]^{2-}$, $[POO_{0/2}O_3]^{3-}$, Na^+ and $(NaSO_4)^-$ free ions (formed by the reaction, $Na_2SO_4 \Leftrightarrow Na^+ + (NaSO_4)^-$); the defects thus produced create easy path ways for the migration of charges that would build up space charge polarization and facilitate to an increase in the dielectric parameters as observed [41–43]. Thus these results also support the view point that there is an increasing degree of disorder in the glass network due to the increasing fraction of Ti^{3+} ions that act as modifiers.

Conventionally, the dielectric relaxation effects are described with the variable frequency at a fixed temperature. However, similar information can also be obtained by analyzing these results at a fixed frequency at variable temperature as suggested by Bottcher and Bordewijk [44].

Substituting Eq. (3) in standard Debye relations for dielectric relaxation, one can obtain

$$\varepsilon'(\omega, T) = \varepsilon_\infty + \tfrac{1}{2}(\varepsilon_s - \varepsilon_\infty)\left[1 - tgh\left(\frac{W_d}{kT + \ln\ \omega A}\right)\right] \quad (5)$$

$$\varepsilon''(\omega, T) = \frac{1/2(\varepsilon_s - \varepsilon_\infty)}{\cosh(W_d/kT + \ln\ \omega A)} \quad (6)$$

In Eqs. (5) and (6), ε_∞ is temperature independent whereas, ε_s is largely dependent on temperature. Keeping the fact in mind that the variation of hyperbolic trigonometric functions in Eqs. (5) and (6) with temperature is very minimal, these equations can be rewritten as

$$\varepsilon'(\omega, T) = \varepsilon_\infty + \frac{1}{2}(\varepsilon_s - \varepsilon_\infty)\left[1 - tgh\left\{\frac{W_d(1/T - 1/T_m(\omega))}{k}\right\}\right] \quad (7)$$

and

$$\varepsilon''(\omega, T) = \frac{1/2(\varepsilon_s - \varepsilon_\infty)}{\cosh[W_d(1/T - 1/T_m(\omega))/k]} \quad (8)$$

In Eqs. (7) and (8), $T_m(\omega)$ is the temperature at where ε' exhibits maximum value. Thus, as per the Eqs. (7) and (8), the plots of $\varepsilon'(\omega, T)$ and $\varepsilon''(\omega, T)$ against $1/T$ should be centro symmetric and symmetric curves, respectively in the dielectric relaxation region. As an example for one of the glass samples (viz., T_{10}) under investigation, the variations of $\varepsilon'(\omega, T)$ and $\varepsilon''(\omega, T)$ with $1/T$ are shown in Fig. 8. The shape of these curves is well in accordance with the Eqs. (7) and (8) and clearly confirms the relaxation character of dielectric properties of these glasses.

With increase in the concentration of TiO_2 an increase in the value of $(\tan\delta)_{max}$ and a shift region of dielectric relaxation towards lower temperature have been noticed. Such variations indicate an increase in the concentration of dipoles that contribute to the relaxation effects. The value of the effective activation energy associated with the dipoles is observed to decrease with increase in the content of TiO_2 in the glass network (Table 4). This observation points out that an increasing freedom for dipoles to orient in the field

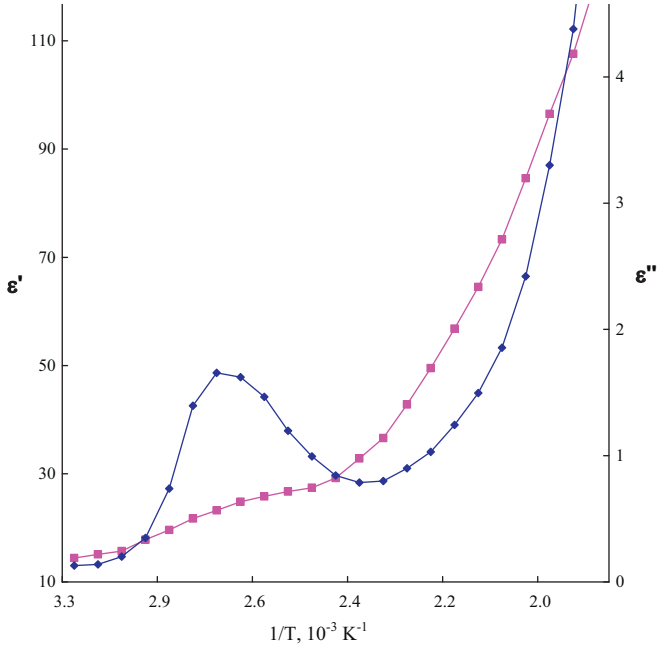

Fig. 8. Variation of ε' and ε'' with $1/T$ at a frequency 10 kHz for the sample T_{10}.

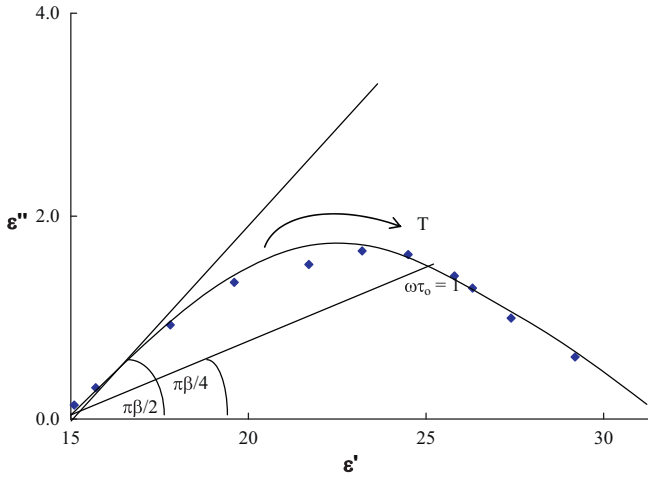

Fig. 9. A pseudo Cole–Cole plot at 10 kHz for the glass sample T_8.

direction. Earlier studies on the glasses containing variety of d^1 ions (like V^{4+}, Mo^{5+}, W^{5+}, Cr^{5+}, etc.,) indicated that the geometrical arrangement of these ions with oxygen form complexes in such a way that they contribute to the dielectric relaxation effects [45–48]; following these arguments, relaxation effects exhibited by the present studied glasses can be attributed to Ti^{3+} (d^1) ion complexes.

Further, to know whether there is single relaxation time or spreading of relaxation times for the dipoles, we have adopted a pseudo Cole–Cole plot method (instead of conventional Cole–Cole plot between $\varepsilon'(\omega)$ and $\varepsilon''(\omega)$ at a fixed temperature) suggested by Sixou et al. [49] in which $\varepsilon'(T)$ vs. $\varepsilon''(T)$ can be plotted at a fixed frequency. The nature of variation of $\varepsilon'(T)$ and $\tan\delta$ with temperature for these glasses indicates that the Cole–Davidson equation:

$$\varepsilon^*(\omega) = \varepsilon_\infty + \frac{\varepsilon_s - \varepsilon_\infty}{(1 + i\omega\tau)^\beta}, \tag{9}$$

can safely be applied to these glasses. Separating real and imaginary terms of Eq. (9), and rewriting with explicit temperature dependence of terms, one can get

$$\varepsilon'(\omega, T) = \varepsilon_\infty + (\varepsilon_s - \varepsilon_\infty)[\cos\ \varphi(T)]^\beta \cos\ \beta\varphi(T) \tag{10}$$

and

$$\varepsilon''(\omega, T) = (\varepsilon_s - \varepsilon_\infty)[\cos\ \varphi(T)]^\beta \sin\ \beta\varphi(T). \tag{11}$$

In Eqs. (10) and (11)

$$\varphi(T) = \tan^{-1}(\omega\tau) = \tan^{-1}(\omega A_o e^{W_d/KT}). \tag{12}$$

In Eq. (12) A_o is a constant and W_d is the activation energy for dipoles. The plot between $\varepsilon'(T)$ and $\varepsilon''(T)$ represented by the Eqs. (10) and (11) at a fixed frequency is often called pseudo Cole–Cole plot, which cuts ε' axis at ε_s and ε_∞. Here, ε_s is known as high temperature dielectric constant (in contrast to the low frequency dielectric constant in the conventional Cole–Cole plot) and similarly ε_∞ is the low temperature dielectric constant. The plot cuts ε' axis at an angle of $(\pi/2)\beta$ at low temperature side (as per Sixou et al. [49]), here β is the spreading factor for relaxation times. For Na_2SO_4–B_2O_3–P_2O_5 glass containing 0.8% of TiO_2 (glass T_8), a pseudo Cole–Cole plot at 10 kHz is shown in Fig. 9. The spreading factor β estimated from this plot is 0.61; such plots have also been drawn for all the glasses and the value of β is estimated in a similar way; the value of β is found to increase gradually with the increase in the concentration of TiO_2 (Table 3). The spreading of relaxation times in these glasses may be understood as due to the experience of an approximately random potential energy by the dipoles on diffusing through the distorted structure of the glass [50,51].

The activation energy associated with ac conductivity is found to decrease with increasing TiO_2 concentration. When $\log\sigma_{ac}$ is plotted against activation energy, W_{ac}, a near linear relationship is found (inset (a) of Fig. 7). This means that the conductivity enhancement is directly related to the thermally stimulated mobility of the charge carriers in the high temperature region. As mentioned earlier, the glasses under study exhibit mixed, ionic and polaronic conductivity. Generally, electronic conduction is due to the polaron hopping between Ti^{3+} and Ti^{4+} ions whereas, ionic conduction is due to migration of Na^+ ions. For these glasses, the ac conductivity increases with increasing content of TiO_2 (Fig. 7). One of the possible explanations for such a behavior is that, the entry of Ti^{3+} ions into the glass network causes to increase the concentration of dangling bonds in the glass network. This in turn leads to decrease in the electrostatic binding energy and the strain energy for the easy passage of conducting ions. Due to these reasons there will be a substantial decrement in the jump distance of Na^+ ions. Such behavior is in good accordance with the observed decrease in activation energy for conduction.

The frequency response of real part of ac conductivity is normally described by power law dependence with '*s*' as exponent:

$$\sigma(\omega) = \sigma_{dc}\left[1 + \left(\frac{\omega}{\omega_c}\right)^s\right], \quad 0 \le s < 1 \tag{13}$$

Indicating, $\sigma(\omega)$ is the sum of the dc conductivity and a fractional power law dependent dispersive conductivity with exponent *s*. Here ω_c is a characteristic crossover frequency from dc to dispersive conductivity.

Within the framework of the linear-response theory, the frequency-dependent conductivity can be related to

$$\sigma(\omega) = -\frac{q^2 n_c \omega^2}{6kTH_R}\int_0^\infty \left\langle r^2(t)\right\rangle e^{-i\omega t}dt \tag{14}$$

where q is the charge, n_c is the mobile ion density, $\langle r^2(t)\rangle$ is the mean square displacement of the mobile ions and H_R is the Haven ratio (lies in between 0.2 and 1.0) [52] which represents the degree of correlation between successive hops.

More precisely, in Eq. (14) $\langle r^2\rangle$ represents the mean squared displacement particles performing random walks on a regular lattice. For excursions shorter than the correlation length the mean squared displacement r^2 varies as a power law t^{1-s}. Under these conditions Eq. (13) modifies to

$$\sigma(\omega) \propto \omega^s \tag{15}$$

with exponent $s < 1$. For the glass T_2, the value of '*s*' (obtained by plotting $\log\sigma(\omega)$ vs. ω (inset (b) of Fig. 7)), is found to be 0.73. With increase in the concentration of TiO_2 the exponent is found to be increasing gradually. In general '*s*' is a measure of the degree of interaction with the environment. In fact this parameter depends on the glass composition and the limit of measurement temperature. The low values of exponent '*s*' (<1) arises from the distribution of the cluster sizes (determined by mutual correlations between dipoles formed in the system) and the distribution of their relaxation rates. Sidebottom while explaining the conduction mechanism in alkali phosphate glasses, concluded that exponent '*s*' depends upon the dimensionality of the local conduction space and it increases with increasing dimensionality [53,54]. Based on these studies the observed increase of '*s*' (inset (c) of Fig. 7) with the concentration of TiO_2 may be attributed to a enhancement in the dimensionality of conducting space with increase in the content of TiO_2 [55].

The low temperature part of the conductivity (a near temperature independent part as in the case of present glasses) up to nearly 70 °C can be explained on the basis of quantum mechanical

tunneling model [56] similar to many other glass systems reported recently [57–59].

5. Conclusions

The glasses of the composition viz., $(40-x)Na_2SO_4$–$30B_2O_3$–$30P_2O_5$: $xTiO_2$ with $0 \le x \le 1.0$ mol% in the steps of 0.2 were synthesized. Dielectric and spectroscopic properties were investigated. The optical absorption and ESR spectral studies revealed the existence of titanium ions in Ti^{3+} state in addition to Ti^{4+} state in the glass network. The IR spectral results indicated the degree of disorder in the glass network increases with the increase in the concentration of TiO_2. The values of dielectric parameters viz., dielectric constant, loss and ac conductivity at any frequency and temperature are observed to increase with the concentration of TiO_2; the increasing space charge polarization is found to be responsible for such an increase. The dielectric relaxation effects exhibited by these glasses are quantitatively analyzed by pseudo Cole–Cole method and the spreading of relaxation times is established. The ac conductivity is observed to increases with increasing content of TiO_2; the mechanism responsible for such increase is well explained based on the modifying action of Ti^{3+} ions.

References

[1] D.A. McKeown, I.S. Muller, H. Gan, I.L. Pegg, C.A. Kendziora, J. Non-Cryst. Solids 288 (2001) 191.
[2] X. Yu, J.B. Bates, G.E. Jellison Jr., F.X. Hart, J. Electrochem. Soc. 144 (1997) 524.
[3] F. Scholz, J. Solid State Electrochem. 15 (2011) 14.
[4] N. Da, O. Grassmé, K.H. Nielsen, G. Peters, L. Wondraczek, J. Non-Cryst. Solids 357 (2011) 2202.
[5] M. Ganguli, M.H. Bhat, K.J. Rao, Solid State Ionics 122 (1999) 23.
[6] I.A. Sokolov, I.V. Murin, V.E. Kriyt, A.A. Pronkin, Glass Phys. Chem. 37 (2011) 351.
[7] V.G. Vyatchina, L.A. Perelyaeva, M.G. Zuev, V.L. Mamoshin, Glass Phys. Chem. 29 (2003) 522.
[8] A.M. Pletnev, R.N. Lapina, O.B. Kozlova, S.G. Bamburov, Glass Phys. Chem. 28 (2002) 1.
[9] B.V.R. Chowdari, K.F. Mok, J.M. Xie, R. Gopalakrishnan, J. Non-Cryst. Solids 160 (1993) 73.
[10] G. Chiodelli, A. Magistris, Solid State Ionics 18 (1986) 356.
[11] R.V. Salokdar, V.K. Deshpande, K. Singh, J. Power Sources 25 (1989) 257.
[12] N.K. Karan, B. Natesa, R.S. Katiyar, Solid State Ionics 177 (2006) 1429.
[13] F. Muñoz, L. Montagne, L. Pascual, A. Durán, J. Non-Cryst. Solids 355 (2009) 2571.
[14] N. Shimoji, T. Hashimoto, H. Nasu, K. Kamiya, J. Non-Cryst. Solids 324 (2003) 50.
[15] E. Golis, I.V. Kityk, J. Wasylak, J. Kasperczyk, Mater. Res. Bull. 31 (1996) 1057.
[16] I.V. Kityk, A. Majchrowski, Opt. Mater. 26 (2004) 33.
[17] A. Shaim, M. Et-tabirou, Mater. Chem. Phys. 80 (2003) 63.
[18] P. Nageswara Rao, C. Laxmi Kanth, D. Krishna Rao, N. Veeraiah, J. Quant. Spectrosc. Radiat. Transfer 95 (2005) 37.
[19] M.J. Weber, R.A. Saroyan, R.C. Ropp, J. Non-Cryst. Solids 44 (1981) 137.
[20] K. Morigaki, Physics of Amorphous Semiconductors, World Scientific, Singapore, 1999.
[21] G. Murali Krishna, Y. Gandhi, N. Veeraiah, Phys. Status Solidi A 205 (2008) 177.
[22] K.J. Rao, Structural Chemistry of Glasses, Elsevier, Amsterdam, 2002.
[23] K. Nakamoto, Infrared Spectra of Inorganic and Coordination Compounds, John Wiley & Sons, New York, 1962.
[24] A. Bhide, K. Hariharan, Mater. Chem. Phys. 105 (2007) 213.
[25] Y. Dimitriev, V. Mihailova, V. Dimitrov, Y. Ivanova, J. Mater. Sci. Lett. 10 (1991) 1249.
[26] A. Shaim, M. Et-Tabirou, Mater. Res. Bull. 37 (2002) 2459.
[27] R. Balaji Rao, D. Krishna Rao, N. Veeraiah, Mater. Chem. Phys. 87 (2004) 357.
[28] B. Tareev, Physics of Dielectric Materials, Mir, Moscow, 1979.
[29] G. Little Flower, M. Srinivasa Reddya, M.V. Ramana Reddy, N. Veeraiah, Z. Naturforsch. 62 (2007) 315.
[30] R.K. Brow, D.R. Tallant, J. Non-Cryst. Solids 222 (1997) 396.
[31] E.T.Y. Lee, E.R.M. Taylor, J. Phys. Chem. Solids 66 (2005) 47.
[32] R.K. Brow, J. Non-Cryst. Solids 194 (1996) 267.
[33] J.J. Videau, J.F. Ducel, K.S. Suh, J. Senegas, J. Alloys Compd. 188 (1992) 157.
[34] N. Da, A.A. Enany, N. Granzow, M.A. Schmidt, P. St, J. Russell, L. Wondraczek, J. Non-Cryst. Solids 357 (2011) 1558.
[35] X.A. Aboukais, L.D. Bogomolova, A.A. Deshkovskaya, V.A. Jachkin Krasil, N.A. Nikova, S.A. Prushinsky, O.A. Trul, S.V. Stefanovsky, E.A. Zhilinskaya, Opt. Mater. 19 (2002) 295.
[36] M.V. Ramachandra Rao, Y. Gandhi, L. Srinivasa Rao, G. Sahayabaskaran, N. Veeraiah, Mater. Chem. Phys. 126 (2011) 58.
[37] O. Cozar, D.A. Magdas, I. Ardelean, J. Non-Cryst. Solids 354 (2008) 1032.
[38] B.V.R. Chowdari, K. Radha Krishnan, J. Non-Cryst. Solids 224 (1998) 151.
[39] I. Abrahams, E. Hadzifejzovic, Solid State Ionics 134 (2000) 249.
[40] B.V. Raghavaiah, C. Laxmikanth, N. Veeraiah, Opt. Commun. 235 (2004) 341.
[41] N. Krishna Mohan, G. Sahaya Baskaran, N. Veeraiah, Phys. Status Solidi A 203 (2006) 2083.
[42] G. Naga Raju, N. Veeraiah, Physica B 373 (2006) 297.
[43] G. Murali Krishna, M. Srinivasa Reddy, N. Veeraiah, J. Solid State Chem. 180 (2007) 2747.
[44] C.J.F. Bottcher, P. Bordewijk, Theory of Electric Polarization, Elsevier, Oxford, 1978.
[45] L. Bih, El. Omari, M. Haddad, J.M. Reau, D. Boudlich, A. Yacoubi, A. Nadiri, Solid State Ionics 132 (2000) 71.
[46] R.M. Abdelouhab, R. Braunstein, K. Baerner, J. Non-Cryst. Solids 108 (1989) 109.
[47] G. Srinivasarao, N. Veeraiah, J. Solid State Chem. 166 (2002) 104.
[48] Y. Gandhi, K.S.V. Sudhakar, M. Nagarjuna, N. Veeraiah, J. Alloys Compd. 485 (2009) 876.
[49] P. Sixou, P. Dansas, D. Gillot, J. Chem. Phys. 64 (1967) 834.
[50] C. Dyre, J. Non-Cryst. Solids 88 (1986) 271.
[51] S.R. Elliott, Physics of Amorphous Materials, Longmen Science and Technology, Essex, 1990.
[52] H. Kahnt, J. Non-Cryst. Solids 203 (1996) 225.
[53] S. Lanfredi, P.S. Saia, R. Lebullenger, A.C. Hernandes, Solid State Ionics 146 (2002) 329.
[54] D.L. Sidebottom, Phys. Rev. Lett. 83 (1999) 983.
[55] S. Bhattacharya, A. Ghosh, Phys. Rev. B 70 (2004) 172203.
[56] I.G. Austin, N.F Mott, Adv. Phys. 18 (1969) 657.
[57] G. Murali Krishna, N. Veeraiah, N. Venkatramaiah, R. Venkatesan, J. Alloys Compd. 450 (2008) 486.
[58] Ch. Srinivasa Rao, V. Ravi Kumar, T. Srikumar, Y. Gandhi, N. Veeraiah, J. Non-Cryst. Solids 357 (2011) 3094.
[59] K. Srilatha, L. Pavić, A. Moguš-Milanković, Ch. Srinivasa Rao, G. Little Flower, V. Ravi Kumar, N. Veeraiah, J. Non-Cryst. Solids 357 (2011) 3538.